The Astrophysical Journal, 600:634–639, 2004 January 10

ARP 299: A SECOND MERGING SYSTEM WITH TWO ACTIVE NUCLEI?

L. Ballo,[1,2] V. Braito,[1,3] R. Della Ceca,[1] L. Maraschi,[1] F. Tavecchio,[1] and M. Dadina[4]

Received 2003 June 10; accepted 2003 September 23

ABSTRACT

Recent *BeppoSAX* observations of Arp 299, a powerful far-IR merging starburst system composed of IC 694 and NGC 3690, clearly unveiled for the first time in this system the presence of a strongly absorbed active galactic nucleus (AGN). However, the system was not spatially resolved by *BeppoSAX*. Here we present the analysis of archival *Chandra* and (for the first time) *XMM-Newton* observations, which allow us to disentangle the X-ray emission of the two galaxies. The detection of a strong 6.4 keV line in NGC 3690 clearly demonstrates the existence of an AGN in this galaxy, while the presence of a strong 6.7 keV Fe-Kα line in the spectrum of IC 694 suggests that this nucleus might also harbor an AGN. This would be the second discovery of two AGNs in a merging system after NGC 6240.

Subject headings: galaxies: active — galaxies: individual (Arp 299, IC 694, NGC 3690) — galaxies: starburst — X-rays: galaxies

1. INTRODUCTION

Arp 299 is a powerful merging system located at $D =$ 44 Mpc (Heckman et al. 1999). The far-IR (FIR) luminosity, $L_{43-123\ \mu\mathrm{m}} = 2.86 \times 10^{11}\ L_{\odot}$, dominates the bolometric output. The system consists of two galaxies in an advanced merging state, NGC 3690 to the west and IC 694 to the east, plus a small compact galaxy to the northwest (Hibbard & Yun 1999). The centers of the two merging galaxies are separated by $\sim 22''$ (Heckman et al. 1999), corresponding to a projected distance of 4.6 kpc. In the IR range, IC 694 shows a compact site of activity in the central region, while NGC 3690 is resolved into a complex of sources without a clear central nucleus (Wynn-Williams et al. 1991; Alonso-Herrero et al. 2000). Optical spectroscopy presented in Coziol et al. (1998) shows that IC 694 can be classified as a pure starburst galaxy, while NGC 3690 has line properties at the borderline between starburst and LINER.

We observed Arp 299 with *BeppoSAX* in the context of a project aimed at investigating the starburst–active galactic nucleus (AGN) connection in relatively nearby systems, where the detection threshold should allow us to detect AGN activity even if not dominant. The observations unveiled for the first time in this system a strongly absorbed AGN ($N_{\mathrm{H}} \simeq 2.5 \times 10^{24}$ cm^{-2}, with an intrinsic luminosity $L_{0.5-100\ \mathrm{keV}} \simeq 1.9 \times 10^{43}$ ergs s^{-1}; Della Ceca et al. 2002). At the spatial resolution of the *BeppoSAX* instruments, however, the system was not resolved, so we were unable to establish in which galaxy the AGN resides.

Arp 299 was the target of both *Chandra* and *XMM-Newton* observations, now available from the archives. Here we present the analysis of these data (those from *XMM-Newton* still unpublished) and discuss the possibility that both galaxies in the interactive system host an AGN. After NGC 6240 (Komossa et al. 2003), this would be the second case of two AGNs in a merging system. In this paper, we assume $H_0 =$ 75 km s^{-1} Mpc^{-1} and $q_0 = 0.5$.

2. OBSERVATIONS AND DATA REDUCTION

Chandra observed Arp 299 on 2001 July 7 for a total of 26.5 ks, corresponding to a net exposure of 24.2 ks. The observation was performed in FAINT mode with the target centered on the aim point S1 of the ACIS-I detector. Screened events produced by the standard pipeline processing (evt2 files) have been used, while data analysis has been performed using the software CIAO version 2.3[5] and the package ds9.[6]

In this work we use the excellent spatial resolution of *Chandra* to have some indication about the origin of the X-ray emission. We show in Figure 1 the X-ray contours obtained from the *Chandra* ACIS-I data in the 0.5–2 keV (Fig. 1*a*), 2–10 keV (Fig. 1*b*), and 6.3–6.9 keV (Fig. 1*c*) energy ranges superimposed on the *Hubble Space Telescope* (*HST*) Wide Field Planetary Camera 2 (WFPC2) image obtained with the F814W filter ($\lambda_{\mathrm{eff}} \simeq 8203$ Å, $\Delta\lambda \simeq 1758.0$ Å).

The *Chandra* 0.5–2 keV emission is clearly extended. Three emission knots are visible within the diffuse emission. The northeast and fainter knot is clearly associated with IC 694, while the other two are associated with NGC 3690. Also the 2–10 keV emission is diffuse, although in this case it is strongly concentrated around the three knots. When observed in the 6.3–6.9 keV energy range (the range where the Fe-Kα line[s], an important spectral signature of an AGN, resides), the strongest sources are clearly localized in two regions associated with the two merging galaxies; moreover, the northwest knot in NGC 3690 disappears.[7]

Arp 299 was observed by *XMM-Newton* on 2001 May 6 for a total of about 20 ks, in full frame mode and with the thin

[1] INAF, Osservatorio Astronomico di Brera, via Brera 28, 20121 Milan, Italy; luballo@brera.mi.astro.it, braito@brera.mi.astro.it, rdc@brera.mi.astro.it, maraschi@brera.mi.astro.it, fabrizio@brera.mi.astro.it.

[2] SISSA/ISAS, International School for Advanced Studies, via Beirut 4, 34014 Trieste, Italy; ballo@sissa.it.

[3] Dipartimento di Astronomia, Università di Padova, Vicolo dell' Osservatorio 2, 35122 Padua, Italy; braito@pd.astro.it.

[4] IASF/CNR, Sezione di Bologna, via Gobetti 101, 40129 Bologna, Italy; dadina@bo.iasf.cnr.it.

[5] See http://cxc.harvard.edu/ciao.

[6] See http://hea-www.harvard.edu/RD/saotng.

[7] While this paper was in the hands of the referee, a detailed spectral and spatial analysis of these *Chandra* data was published in Zezas, Ward, & Murray (2003).

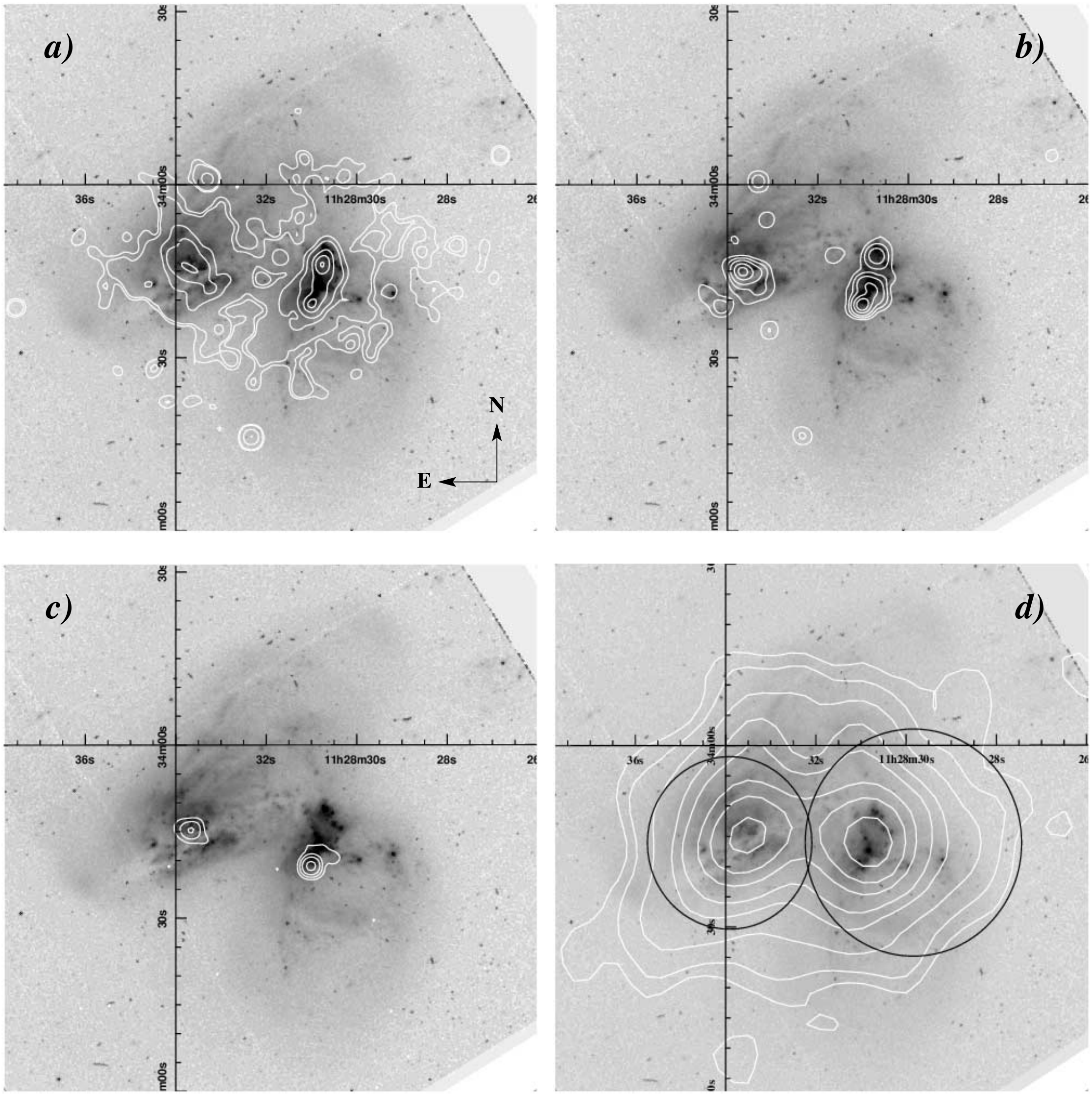

Fig. 1.—X-ray contours derived (using a Gaussian smoothing point-spread function [PSF] with a FWHM of 1 pixel, i.e., comparable with the *Chandra* PSF) from the *Chandra* ACIS-I data in different energy ranges superimposed on the *HST* WFPC2 image; (*a*) 0.5–2 keV (contours corresponding to 0.13, 0.319, 0.634, 1.264, 3.154, 4.729, and 6.304 counts pixel^{-1}; the mean background is 0.004 counts pixel^{-1}), where we detected 284 ± 17, 468 ± 22, and 307 ± 18 net counts within a radius of 3″ from the emission peaks of the eastern, northwestern, and southwestern knots, respectively; (*b*) 2–10 keV (contours corresponding to 0.24, 0.51, 0.96, 1.86, and 2.76 counts pixel^{-1}; the mean background is 0.06 counts pixel^{-1}), where the net counts close ($r < 3''$) to the emission peaks are 116 ± 11, 73 ± 9, and 165 ± 13; (*c*) 6.3–6.9 keV (contours corresponding to 0.03834, 0.09534, 0.19034, and 0.38034 counts pixel^{-1}; the mean background is 0.00034 counts pixel^{-1}), with net counts of 6 for the eastern source and 15 for the western one; and (*d*) *XMM-Newton* EPIC-pn contours of Arp 299 in the 0.5–10 keV band, corresponding to 3 σ, 5 σ, 10 σ, 20 σ, 30 σ, 50 σ, 70 σ, and 100 σ, superimposed on the same image; the circles mark the regions considered for the spectral analysis.

filter applied. We used only European Photon Imaging Camera (EPIC) pn data since the MOS data are of insufficient quality above 6 keV. The *XMM-Newton* data have been cleaned and processed using the Science Analysis Software (SAS ver. 5.4) and analyzed using standard software packages (FTOOLS ver. 4.2, XSPEC ver. 11.2). Event files produced from the standard pipeline processing have been filtered for high-background time intervals, and only events corresponding to patterns 0–4 have been used (see the *XMM-Newton* Users' Handbook[8]); the net exposure time after data cleaning is ~14 ks. The latest calibration files released by the EPIC team have been used. We have also generated our own response matrices at the position of the system using the SAS tasks *arfgen* and *rmfgen*. No statistically significant source variability has been detected during the *XMM-Newton* observation.

The *XMM-Newton* image in the 2–10 keV energy range shows two sources of comparable brightness corresponding to the two interacting galaxies. To compare the EPIC-pn spectrum with that obtained by *BeppoSAX* we extracted the source counts from a circular region of radius 28″.5, including the whole merging system. The background spectrum was extracted from a nearby source-free circular region of ~79″ radius. The net count rate (0.5–10 keV energy range) of the total merging system is 0.4822 ± 0.0063 counts s^{-1}; it represents about 98.8% of the total counts in the source extraction region. To perform the spectral analysis, source counts were rebinned to have a number of counts greater than 20 in each energy bin.

[8] See http://xmm.vilspa.esa.es/external/xmm_user_support/documentation/uhb_2.0/index.html.

In order to derive the spectra of the two sources separately, we selected two smaller regions centered at their X-ray centroid positions (IC 694: R.A. = $11^h28^m33^s.9$, decl. = $+58°33'43''.9$; NGC 3690: R.A. = $11^h28^m29^s.8$, decl. = $+58°33'43''.9$). In the case of NGC 3690, the spectrum was extracted from a circle of radius $18''.75$ (limited in size by the presence of the other nucleus). For IC 694 we used a smaller radius of $14''.25$ because of the proximity of the CCDs' gap. The extraction regions are shown in Figure 1*d*. The background spectra were extracted from two source-free circular regions close to the individual sources of radius $32''.5$ and $27''.5$, respectively. The net count rate (0.5–10 keV energy range) of IC 694 (NGC 3690) is 0.1686 ± 0.0044 counts s^{-1} (0.2291 ± 0.0049 counts s^{-1}) and represents about 97.5% (98.3%) of the total counts in the source extraction region. Source counts have been rebinned to have a number of counts greater than 10 in each energy bin.

All the models discussed here have been filtered through the Galactic absorption column density along the line of sight ($N_{\rm H,\,Gal} = 9.92 \times 10^{19}$ cm^{-2}; Dickey & Lockman 1990); all the errors are at 90% confidence level for 1 parameter of interest ($\Delta\chi^2 = 2.71$). The reported line positions refer to the source rest frame; the metallicity of the thermal component(s) used was fixed to the solar value.

3. SPECTRAL ANALYSIS

3.1. *The Whole System: Comparison with Previous BeppoSAX Results*

Arp 299 was observed by *BeppoSAX* about 7 months after the observations of *XMM-Newton*; the *BeppoSAX* MECS and *XMM-Newton* EPIC-pn 2–10 keV fluxes obtained assuming a simple power-law model are comparable within the uncertainties. In order to check the consistency of our previous results, the *XMM-Newton* EPIC-pn spectrum of the whole Arp 299 system (see previous section) was analyzed jointly with the *BeppoSAX* data. We fitted the data in the 0.3–40 keV energy range with the *BeppoSAX* best-fit model (see Della Ceca et al. 2002 for details), composed of a soft thermal component, a "leaky-absorber" model (an unabsorbed power law + an absorbed power law with the same photon index Γ), and two Gaussian emission lines (at $E \sim 6.4$ and 3.4 keV, respectively). The LECS to MECS and PDS to MECS normalization factors were allowed to vary in the range suggested by the *BeppoSAX* Cookbook.[9]

The ratio of *XMM-Newton* EPIC-pn data to the best-fit model discussed above shows a deficit of photons at $E < 0.8$ keV, which was present but not statistically significant in the *BeppoSAX* data (because of the poor LECS statistics at low energies). This requires additional absorption in front of the soft thermal component, with a column density of $N_{\rm H,\,soft} \sim 1.5 \times 10^{21}$ cm^{-2} (consistent with the absorption found for several Seyfert 2 galaxies with circumnuclear starbursts; see Levenson, Weaver, & Heckman 2001a, 2001b). With this modification, the overall model proposed by Della Ceca et al. (2002) well reproduces the *XMM-Newton* + *BeppoSAX* data; the values found for the most relevant parameters ($N_{\rm H,hard} \sim 2.6 \times 10^{24}$ cm^{-2}, $\Gamma \sim 1.89$, $kT \sim 0.64$ keV, $E \sim 6.41$ keV, and $\chi^2/{\rm dof} = 607.1/542$) are in good agreement with those previously obtained. This global modeling of Arp 299 is also a good fit of the *XMM-Newton* EPIC-pn data only, with the only exception that the presence of a Gaussian line at 3.4 keV is not required. The absorbed fluxes and the intrinsic (i.e., unabsorbed) luminosity are consistent with our previous results, confirming our earlier conclusion about the presence of a deeply buried AGN in the system.

3.2. *X-Ray Emission from the Two Galaxies*

Using only the EPIC-pn data, we have studied the X-ray emission produced by the two merging galaxies. Their 0.5–10 keV band emission can be well described by a thermal component + a power law + a Gaussian emission-line model, with soft X-ray absorption in addition to the Galactic one. Apart from the energy and equivalent width (EW) of the emission lines (see below), the best-fit parameters are very similar for the two galaxies ($kT \sim 0.66$ keV, $\Gamma \sim 1.9$, and $N_{\rm H,\,soft} \sim 1.5 \times 10^{21}$ cm^{-2}). Furthermore, the two galaxies contribute to the observed 2–10 keV emission of Arp 299 with similar intensities.

As expected, at energies lower than 2 keV the dominant contribution is due to the thermal emission associated with the starburst component. The luminosity of this thermal component is $L_{0.5-2\,\rm keV} = 1.37 \times 10^{41}$ ergs s^{-1} for NGC 3690 and $L_{0.5-2\,\rm keV} = 1.08 \times 10^{41}$ ergs s^{-1} for IC 694.

In order to study the nuclear X-ray emission of NGC 3690 and IC 694, we now concentrate on the 2–10 keV energy range, where the contribution from the soft thermal component is negligible. In Figure 2 (*top panels*) we show the ratio of the *XMM-Newton* data to a single unabsorbed power-law fit ($\Gamma = 1.89$ for NCG 3690 and $\Gamma = 1.97$ for IC 694); for both of these sources, the residuals suggest the presence of linelike features at energies between 6.3 and 7 keV. In fact, by adding a Gaussian emission line to the simple power-law model in both cases, the fit improves significantly according to the *F*-test; the results of our analysis are reported in Table 1 and are shown in Figure 2 (*middle and bottom panels*). From our fit, the main difference between the two objects is the position and the EW of the emission lines. In the case of IC 694, the energy of this feature is consistent with He-like Fe-Kα, while in the case of NGC 3690 the energy is consistent with Fe-Kα from neutral Fe.

4. DISCUSSION

In the following section we discuss the implications of the spectral analysis previously described, focusing on the location of the deeply buried AGN in this system, as we know from *BeppoSAX* observation. Because of the absorbing column density observed by *BeppoSAX* ($\sim 2.5 \times 10^{24}$ cm^{-2}), the direct X-ray continuum from the obscured AGN can be see only at energies greater than 10 keV. So in the energy range covered by *XMM-Newton*, it is completely absorbed; the only observable and clear signature of this AGN is a cold Fe-Kα line with high EW, as expected if produced by transmission through the neutral material responsible for the absorption measured by *BeppoSAX*. Such a line is clearly detected in the *XMM-Newton* spectrum of NGC 3690, strongly arguing for the presence in this galaxy of the absorbed AGN inferred from the *BeppoSAX* observation. Assuming that NGC 3690 produces the whole hard X-ray flux observed by the *BeppoSAX* PDS, the continuum observed by *XMM-Newton* in the 2–10 keV energy range is only $\sim$2% of the intrinsic one. This continuum is probably due to a combination of emission from sources related to the starburst (e.g., X-ray binaries) and/or reprocessed AGN emission (reflection and/or scattering)

[9] See http://ftp.asdc.asi.it/pub/software_docs/saxabc_v1.2.ps.gz.

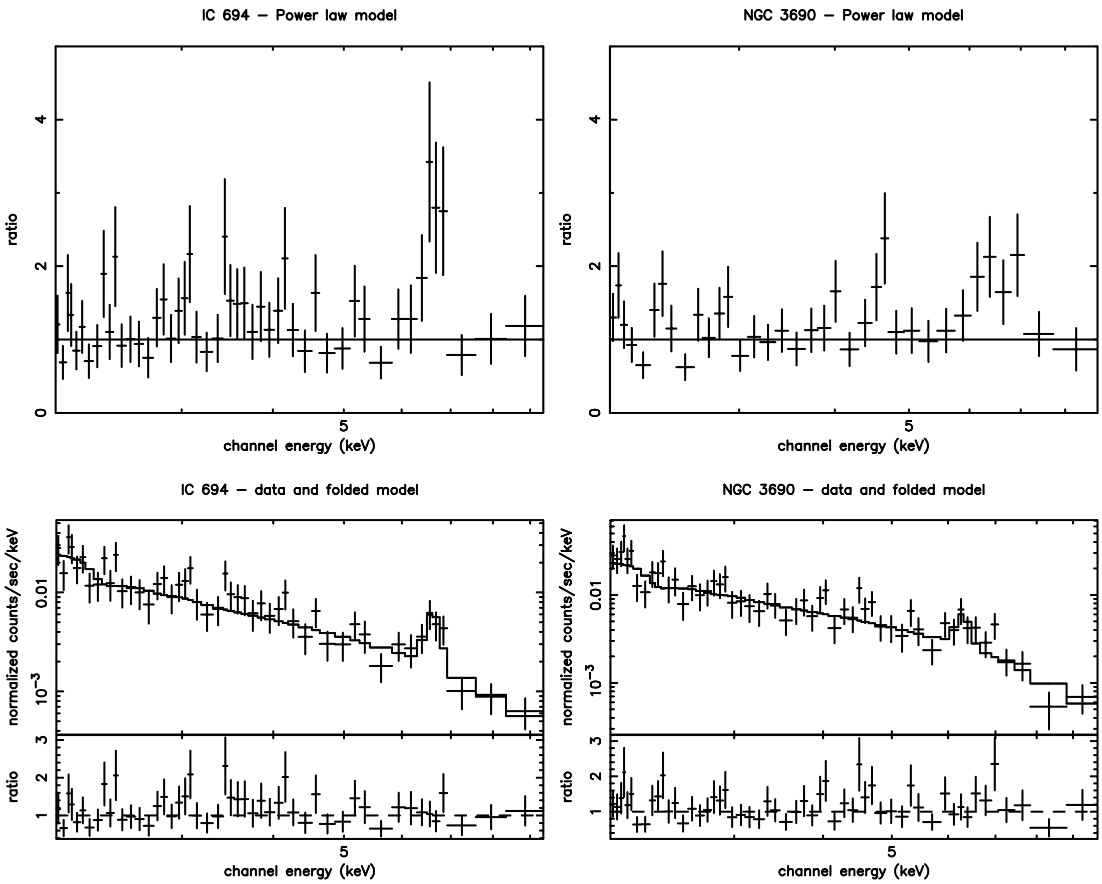

Fig. 2.—Results of the *XMM-Newton* EPIC-pn data for IC 694 (*left*) and NGC 3690 (*right*) fitted with different models. *Top panels*: Ratio of a simple power-law model to the data. For demonstration purposes, data of NGC 3690 have been binned to have a number of counts greater than 15 in each energy bin. *Middle panels*: Data and folded spectra for a fit with a power-law component and a Gaussian line. *Bottom panels*: Ratio of the data to the power law+Gaussian line model.

to our line of sight. The *XMM-Newton* data do not allow us to disentangle these different contributions.

The case of IC 694 is more ambiguous, since the 6.7 keV line from highly ionized Fe could be produced by a high-temperature thermal plasma. In fact, we have been able to reproduce the 2–10 keV spectrum of IC 694 (continuum+line) using a combination of a cutoff power-law model (reproducing the integrated emission of X-ray binaries; see Persic & Rephaeli 2002) and a thermal (MEKAL) model with $kT \simeq 5.5$ keV; the two components are linked so as to reproduce the fraction of X-ray emission assigned by *Chandra* to discrete sources (Zezas, Ward, & Murray 2003). During the fit the slope of the cutoff power-law model was constrained to vary between 1.3 and 1.5, while we fixed the cutoff energy to $E = 8$ keV. The resulting temperature is higher than the values typically found in supernova remnants (SNRs) but consistent with that found, for instance, in the SNR N132D by Behar et al. (2001). Assuming a typical X-ray luminosity of young SNRs of $L_{\rm X} \sim 10^{37}$ ergs s^{-1} and a typical duration of the hot phase of 1000 yr (see . Persic & Raphaeli 2002 for a detailed discussion on this topic), the measured 2–10 keV thermal luminosity of IC 694 ($\sim 6.5 \times 10^{40}$ ergs s^{-1}) implies about 6500 SNRs in the nuclear starburst and a supernovae rate of 6.5 yr^{-1}; the latter value is about a factor of 10 larger than the supernovae rate estimated in the central part of IC 694 ($<5''$, where the bulk of the 2–10 keV emission is produced; see Fig. 1*b*) from radio and near-IR observations (Alonso-Herrero et al. 2000).[10] Thus, although the data do not definitively rule out the starburst origin of the emission line, this possibility implies rather extreme conditions (number of SNRs and high plasma temperature).

In spite of the fact that the luminosity of the Fe-Kα emission line might depend on several ambient factors, a comparison with starburst galaxies showing such a line can, however, supply some information about the expected line intensity. We note that among "pure" starburst galaxies, the He-like Fe line at $E \sim 6.7$ keV with an EW comparable to that of IC 694 is firmly detected only in NGC 253.[11] In order to compare our results with those obtained with *Chandra* for NGC 253 (Weaver et al. 2002), we estimated the central ($\sim 5''$) FIR luminosity of IC 694 using the radio measurement at 1.4 GHz (taken from the Faint Images of the Radio Sky at Twenty cm [FIRST] survey[12]) and the well-known radio/IR correlation for star-forming galaxies (Condon 1992). We have rescaled the Fe line luminosity of NGC 253 reported by Weaver et al. (2002)

[10] We also tried a fit leaving the intensity of the binary cutoff power-law model free to vary. In this case, the supernovae rate implied by the best-fit luminosity is 7.3 yr^{-1}. Similar results have been obtained, leaving free also the slope and the cutoff energy.

[11] The only other starburst galaxy that shows a line from highly ionized Fe is M82, but its EW is significantly lower than that measured here (Cappi et al. 1999; Rephaeli & Gruber 2002).

[12] See http://sundog.stsci.edu.

TABLE 1

RESULTS OF THE SPECTRAL ANALYSIS (EPIC-pn 2–10 keV): PARTIALLY ABSORBED POWER LAW+NARROW GAUSSIAN LINE

	Power Law		Line						
	Γ	Norm.[a]	E (keV)	Norm.[b]	EW (eV)	$N_{\mathrm{H,\,soft}}$[c] (10^{21} cm^{-2})	Flux[d] (10^{-13} ergs cm^{-2} s^{-1})	Luminosity[e] (10^{41} ergs s^{-1})	χ^2/dof
IC 694	1.95 ± 0.20	$1.52^{+0.43}_{-0.32}$	$6.69^{+0.12}_{-0.09}$	$3.02^{+1.40}_{-1.46}$	818^{+380}_{-396}	2.35	4.33	1.02	40.62/45
NGC 3690[f].....	$1.80^{+0.44}_{-0.32}$	$1.29^{+1.46}_{-0.49}$	$6.36^{+0.27}_{-0.14}$	$1.92^{+1.20}_{-1.31}$	422^{+262}_{-288}	5.56	4.37	1.06	50.45/50

NOTES.—Errors are quoted at the 90% confidence level for 1 parameter of interest ($\Delta\chi^2 = 2.71$). The net count rate in the 2–10 keV energy range is 0.0363 ± 0.0031 counts s^{-1} for IC 694 and 0.0401 ± 0.0031 counts s^{-1} for NCG 3690 (about 97.6% and 97.3% of the total counts, respectively).

[a] In units of 10^{-4} photons keV^{-1} cm^{-2} s^{-1} at 1 keV.

[b] In units of 10^{-6} photons keV^{-1} cm^{-2} s^{-1} in the line.

[c] Column density of neutral hydrogen in addition to $N_{\mathrm{H,\,Gal}} = 9.92 \times 10^{19}$ cm^{-2}.

[d] Observed X-ray fluxes.

[e] Observed X-ray luminosities.

[f] The line profile appears marginally broad ($\sigma = 0.32^{+0.64}_{-0.25}$ keV). This can be due to the blending of several lines: if the 2–10 keV continuum is produced by a "warm mirror" that scatters the primary radiation of the central source, then we would expect emission lines from highly ionized Fe. A second linelike feature seems to be present at higher energies ($E \sim 7$ keV), but the present statistics preclude firm conclusions.

using the ratio of the FIR luminosities of the two galaxies, and we have found that the starburst emission could account for about 20% of the observed line intensity in IC 694. Note that also NGC 253 may harbor a hidden AGN, as suggested by some authors (see, e.g., Mohan, Anantharamaiah, & Goss 2002).

So (as also suggested on the basis of its radio properties; see Gehrz, Sramek, & Weedman 1983), there is a strong possibility that in the nucleus of IC 694, an AGN may be present. In this case, the presence of an He-like Fe-Kα emission line suggests that the AGN continuum could be scattered/reflected by a highly ionized gas. A similar emission line (not accompanied by a cold Fe-Kα line) has been recently found by *XMM-Newton* in the FR I galaxy NGC 4261 (Sambruna et al. 2003).

Indeed, we tried to model the spectrum with a reflected component as described by Ross & Fabian (1993; available in XSPEC as a *table* model file[13]). Since the predicted continuum due to reflection by an ionized slab can be characterized by features at low energies, we considered the full 0.5–10 keV spectrum, adding a MEKAL thermal component at low energies to take into account the starburst contribution. This model accounts quite well for the entire spectrum (χ^2/dof = 201.6/183) and can reproduce the Fe-Kα line with physically acceptable values for the main parameters: $kT \sim 0.2$ keV, $\Gamma \sim 2$, and an ionization parameter[14] $\xi = 2.6 \times 10^3$.

The absence of a neutral Fe-Kα line and the lack of any sign of absorption due to a medium with high column density indicate that the AGN inside IC 694 is not heavily absorbed ($N_{\mathrm{H}} \leq 10^{22}$ cm^{-2}). The observed 2–10 keV radiation is probably the direct emission of the central source, an AGN of low luminosity ($L_X \sim 10^{41}$ ergs s^{-1}) surrounded by a cloud of highly ionized gas. The most probable reason that prevents us from identifying IC 694 as an AGN from optical spectroscopic observations is the strong circumnuclear starburst (note that the FIR luminosity is about 3 orders of magnitude greater than the X-ray luminosity of the AGN; see Charmandaris, Stacey, & Gull 2002), which could dilute its optical light (see, e.g., Georgantopoulos, Zezas, & Ward 2003).

To conclude, although a starburst origin of the X-ray emission observed in IC 694 cannot be ruled out, the most plausible hypothesis to explain the X-ray data presented here seems to be the existence of an AGN in each merging galaxy, one highly absorbed ($N_{\mathrm{H}} \simeq 2.5 \times 10^{24}$ cm^{-2}) and of high luminosity ($L_{0.5-100\ \mathrm{keV}} \simeq 1.9 \times 10^{43}$ ergs s^{-1}), the other one less luminous ($L_{2-10\ \mathrm{keV}} \simeq 10^{41}$ ergs s^{-1}) and surrounded by highly ionized gas. In order to establish the AGN activity in IC 694, hard (>10 keV) X-ray observations with angular resolution sufficient to disentangle the X-ray emission from the two galaxies would be needed. Such observations are far to come (Constellation X). Longer and/or repeated *XMM-Newton* observations, providing information on the variability of the X-ray sources, would be at the moment the only means to test the AGN hypothesis for IC 694.

This research was based on observations obtained with *XMM-Newton*, funded by ESA Member States and the US (NASA). We thank A. Celotti and M. Cappi for useful comments. This work received partial financial support from ASI (I/R/037/01, I/R/062/02, and I/R/047/02) and MURST (Cofin 2001). We thank the referee, A. Zezas, for useful comments and suggestions that have substantially improved the paper.

[13] See http://heasarc.gsfc.nasa.gov/docs/xanadu/xspec/models/iondisc.html.

[14] Here $\xi \equiv L_{\mathrm{ill}}/(nR^2)$, where L_{ill} is the luminosity of the continuum, n is the numerical density (part cm^{-3}) of the illuminated slab, and R is the distance between the slab and the illuminating source.

REFERENCES

Alonso-Herrero, A., Rieke, G. H., Rieke, M. J., & Scoville, N. Z. 2000, ApJ, 532, 845
Behar, E., Rasmussen, A. P., Griffiths, R. G., Dennerl, K., Audard, M., Aschenbach, B., & Brinkman, A. C. 2001, A&A, 365, L242
Cappi, M., et al. 1999, A&A, 350, 777
Charmandaris, V., Stacey, G. J., & Gull, G. 2002, ApJ, 571, 282
Condon, J. J. 1992, ARA&A, 30, 575
Coziol, R., Torres, C. A. O., Quast, G. R., Contini, T., & Davoust, E. 1998, ApJS, 119, 239
Della Ceca, R., et al. 2002, ApJ, 581, L9
Dickey, J. M., & Lockman, F. J. 1990, ARA&A, 28, 215
Gehrz, R. D., Sramek, R. A., & Weedman, D. W. 1983, ApJ, 267, 551
Georgantopoulos, I., Zezas, A., & Ward, M. J. 2003, ApJ, 584, 129
Heckman, T. M., Armus, L., Weaver, K. A., & Wang, J. 1999, ApJ, 517, 130
Hibbard, J. E., & Yun, M. S. 1999, AJ, 118, 162
Komossa, S., Burwitz, V., Hasinger, G., Predehl, P., Kaastra, J. S., & Ikebe, Y. 2003, ApJ, 582, L15

Levenson, N. A., Weaver, K. A., & Heckman, T. M. 2001a, ApJS, 133, 269
———. 2001b, ApJ, 550, 230
Mohan, N. R., Anantharamaiah, K. R., & Goss, W. M. 2002, ApJ, 574, 701
Persic, M., & Rephaeli, Y. 2002, A&A, 382, 843
Rephaeli, Y., & Gruber, D. 2002, A&A, 389, 752
Ross, R. R., & Fabian, A. C. 1993, MNRAS, 261, 74
Sambruna, R. M., Gliozzi, M., Eracleous, M., Brandt, W. N., & Mushotzky, R. 2003, ApJ, 586, L37
Weaver, K. A., Heckman, T. M., Strickland, D. K., & Dahlem, M. 2002, ApJ, 576, L19
Wynn-Williams, C. G., Hodapp, K.-W., Joseph, R. D., Eales, S. A., Becklin, E. E., McLean, I. S., Simons, D. A., & Wright, G. S. 1991, ApJ, 377, 426
Zezas, A., Ward, M. J., & Murray, S. S. 2003, ApJ, 594, L31